Enhancing Lightpath QoT Computation with Machine Learning in Partially Disaggregated Optical Networks

Received 14 January 2021; revised 26 February 2021; accepted 10 March 2021.
Date of publication 19 March 2021; date of current version 30 March 2021.

Digital Object Identifier 10.1109/OJCOMS.2021.3066913

Enhancing Lightpath QoT Computation With Machine Learning in Partially Disaggregated Optical Networks

ANDREA D'AMICO [1] (Graduate Student Member, IEEE), STEFANO STRAULLU [2], GIACOMO BORRACCINI [1] (Graduate Student Member, IEEE), ELLIOT LONDON [1] (Graduate Student Member, IEEE), STEFANO BOTTACCHI [3], STEFANO PICIACCIA [4], ALBERTO TANZI [4], ANTONINO NESPOLA [2], GABRIELE GALIMBERTI [4], SCOTT SWAIL [3], AND VITTORIO CURRI [1] (Senior Member, IEEE)

[1] Dipartimento di Elettronica e Telecomunicazioni, Politecnico di Torino, 10129 Turin, Italy

[2] Optical Communications and Networking, Istituto Superiore Mario Boella, 10138 Turin, Italy

[3] Optical Transport, Lumentum, San Jose, CA 95131, USA

[4] Cisco Photonics, Cisco, 20871 Vimercate, Italy

CORRESPONDING AUTHOR: A. D'AMICO (e-mail: andrea.damico@polito.it)

This work was supported by Cisco and has received funding from the European Union Horizon 2020 Research and Innovation Programme under the Marie Skłodowska-Curie Grant under Agreement 814276.

ABSTRACT Increasing traffic demands are causing network operators to adopt disaggregated and open networking solutions to better exploit optical transmission capacity, and consequently enable a software-defined networking (SDN) approach to control and management that encompasses the WDM data transport layer. In these frameworks, a quality of transmission estimator (QoT-E) that gives the generalized signal-to-noise ratio (GSNR) is commonly used to compute the feasibility of transparent lightpaths (LP)s, taking into account the amplified spontaneous emission (ASE) noise and the nonlinear interference (NLI). In general, the ASE noise is the main contributor to the GSNR and is also the most challenging noise component to evaluate in a scenario with varying spectral loads, due to fluctuations in the optical amplifier responses. In this work, we propose a machine learning (ML) algorithm that is trained using different ASE-shaped spectral loads in order to predict the OSNR component of the GSNR; this methodology is subsequently used in combination with a QoT-E in the lightpath computation engine (L-PCE). We present an experiment on a point-to-point optical line system (OLS), including 9 commercial erbium-doped fiber amplifiers (EDFA)s used as black-boxes, each with variable gain and tilt values, and 8 fibers that are characterized by distinct physical parameters. Within this experiment, we receive the signal at the end of the OLS, measuring the bit-error-rate (BER) and the power spectrum, over 2520 different spectral loads. From this dataset, we extract the expected GSNRs and their linear and nonlinear components. Through joint application of a ML algorithm and the open-source GNPy library, we obtain a complete QoT-E, demonstrating that a reliable and accurate LP feasibility predictor may be implemented.

INDEX TERMS Machine learning, optical communications, erbium doped fiber amplifier (EDFA), Raman scattering, quality of transmission (QoT).

I. INTRODUCTION

AS CAPACITY and traffic demands continue to increase [1], network operators have started to look towards innovative solutions that exploit existing infrastructures, in order to maximally increase transmission speeds and capacities [2], [3]. In particular, disaggregated and open infrastructures have been identified as solutions that afford networks with greater degrees of flexibility and allow

multi-vendor approaches to be realized [4]–[6]. In these regimes, a software-defined networking (SDN) approach to optical network control and management may be implemented, with lightpaths (LP)s being assigned dynamically. This allows the wavelength division multiplexed (WDM) optical transport to be implemented in a fully virtual fashion with a common application programming interface (API), in order to independently manage network subsystems and components [7]. To achieve this, a quality of transmission estimator (QoT-E) must be used to compute the generalized signal-to-noise ratio (GSNR) of transparent LPs to assess network performance before, after and during deployment, enabling implementation of the lightpath computation engine (L-PCE). Operating under the assumption that LPs are additive white Gaussian noise (AWGN) channels, the GSNR includes the accumulations of both the amplified spontaneous emission (ASE) noise that arises from the amplifiers, and the nonlinear interference (NLI) noise that is induced by the fiber propagation [8], with the interaction between these two contributions being negligible in terrestrial networks [9], [10]. This approach has been extensively validated, in particular a reliable QoT estimation is provided by the open-source GNPy project [11], which is able to accurately simulate these propagation impairments with a small computational overhead, given sufficient information about the system under investigation [12], [13].

To prevent downtime, network operators must ensure that the QoT never falls below a given lower bound, which has led to the implementation of design margins that quantify uncertainties on the QoT degradation. In many cases these margins have risen to multiple dB as a result of conservative overestimations [14] – reducing the uncertainties contributing to these margins may enable a significant traffic increase without any changes to the network configuration. An overview of the various classifications of margins and their contributors is presented in [15]. In this work, we consider a partially disaggregated optical network with a SDN approach to control and management [16], [17]; the network is constructed from disaggregated re-configurable optical add-drop multiplexers (ROADM)s [4], [18], connected by independent optical line systems (OLSs) that include the degrees of the ROADM multiplexer/demultiplexer, fibers, and amplifiers (booster, in-line and pre-amp). These OLSs transport colored WDM optical tributary signals [19] from ROADM to ROADM upon transparent LPs, with each OLS independently orchestrated using the SDN controller [20]. In this framework any LP can be separated into the OLSs that are traversed during signal propagation; crucially, the total QoT may be calculated using the knowledge of each QoT contribution arising from these OLSs. We focus our study on estimating the GSNR over one of these domains and investigating the fluctuations in signal quality that arise when varying the spectral load.

In general, the main contributor to the LP QoT degradation is the ASE noise [21], [22], which depends on the working points of the erbium-doped fiber amplifiers (EDFA)s within the OLSs. Given the different signal power dependencies of the ASE and NLI contributions, in an optimal working point scenario the former is the most significant contributor to the GSNR degradation, as it is twice the NLI. Minimizing the uncertainty on ASE noise is an ideal target for margin reduction, as its magnitude depends upon the spectral load, which includes non-trivial effects such as spectral hole burning [23], [24]. A naive characterization of the amplifiers to find these ASE noise contributions would require investigation of all plausible spectral load configurations before the LP is established, which is unfeasible for almost all practical scenarios. Instead, this problem represents an ideal scenario for the application of machine learning (ML), allowing the relation between the ASE noise generated by amplifiers present within the LP for each spectral load to be deduced, subsequently enabling the design margin to be significantly reduced. This may be achieved by collecting a dataset of the OLS responses to various spectral loads in order to train a ML algorithm, allowing a QoT-E to be calculated for both untested spectral load configurations and LPs which have not yet been explored. Subsequently, this ML approach may be combined with a sufficiently accurate QoT-E that accounts for NLI contributions – in this way, the QoT impairments that are produced when a new LP is established may be accurately predicted for arbitrary spectral load configurations.

In this work we perform an experimental validation of this methodology, obtaining the GSNR at the termination of a non-transparent, point-to-point optical amplified line, containing 9 erbium-doped fiber amplifiers (EDFA)s, each with distinct but fixed gain and tilt values, and 8 fibers, each distinguished by a unique set of physical parameters. Besides the GSNR measurements, we also measure the signal and ASE noise powers at the termination of the OLS, obtaining a dataset that is used to train a deep neural network (DNN) over 2520 different measured spectral loads – providing OSNR predictions that may be used to reduce uncertainties that arise from amplifier response fluctuations. Combining these OSNR predictions with an accurate model of the NLI implemented in the GNPy engine provides a precise estimation of the total GSNR within the OLS under consideration.

This work is organized as follows: In Section II an overview of related works is presented. In Section III we outline the fundamental network architecture under consideration, along with the approach to QoT-E calculation. In Section IV we describe the experimental setup and the campaign that has been undertaken. In Section V we describe the characterization of the OLS components. In Section VI we report the settings chosen for the ML model and a conceptual overview of the ML application is given. In Section VII we present the results of our investigation. In Section VIII we provide comments regarding the outcome of this work and describe future investigations.

II. RELATED WORK

Establishing a new LP with the lowest possible margin requires an accurate QoT-E, regardless of the spectral load

configuration. Various ML approaches have been investigated and compared for this purpose, ranging from a general QoT estimation perspective to more accurately quantifying individual margin contributions. Considering first the former, there has been much research showing the ability of ML techniques to produce sufficiently accurate results. Initial works, with [25] given as an example, have provided a methodological framework where the bit-error-rate (BER) of an LP may be supplied to a cognitive estimator in order to classify its feasibility. More recent works have adapted this methodology, now encompassing a wide variety of scenarios. In [26] LP feasibility is investigated using margin thresholds, with a ML algorithm used to predict the BERs of new LPs. In [27] a k-nearest-neighbor (KNN) algorithm is used to predict whether a planned LP within a model network can be successfully implemented for a variety of modulation formats and bandwidth occupancies. In [28] supervised ML models are used to accurately predict uncertainties in physical- and network-layer impairments for the Deutsche Telekom (DT) and NSFnet topologies. An implementation which is able to predict the OSNR of new lightpaths with microsecond speeds has also been demonstrated [29]. The performance of various ML algorithms for these purposes has also been compared, with [30] showing that artificial neural networks (ANN)s may provide the highest level of accuracy. We remark that extensive surveys of existing ML approaches applied to optical networking have already been performed and may be found in [31]–[33].

Focusing specifically on the quantification of EDFA uncertainties for margin reduction purposes, ML has previously been utilized to model EDFA gain [34], [35], noise figures [36], [37] and power excursions [38], [39], with [39] further demonstrating wavelength assignment using an algorithm that was able to recommend channel provisioning based upon the ML model results. Correction for EDFA gain ripple has also been targeted in [40], [41], with [41] further using monitoring information to significantly reduce the margin of a network planning tool based upon the Gaussian noise (GN) model. Some recent works have moved beyond predicting ASE noise contributions in isolation; a hybrid approach is investigated in [42], demonstrating that the performance of common ML implementations may be enhanced by inclusion of an analytical model of EDFA gain. The improvement in ML predictions when considering a nonlinear transmission model has also been demonstrated in [43].

The ML implementation within this work is performed in a similar way to a previous work [44], where a deep neural network (DNN) implemented within the TensorFlow open source library [45] is used to estimate the OSNR of arbitrary new lightpaths. We go beyond both this previous work and other recent works described within this section in multiple ways. We provide a study of the overall GSNR built from two constituent models; with the NLI contribution being modelled with an accurate QoT-E – the GNPy engine, and the OSNR contribution being predicted using two

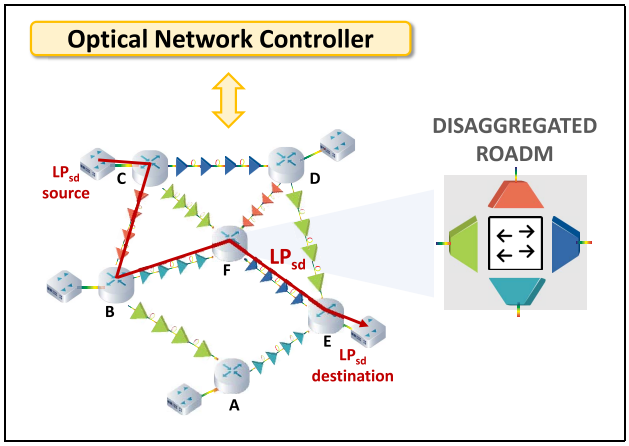

FIGURE 1. A partially disaggregated optical network that deploys independent OLSs on ROADM-to-ROADM WDM optical lines.

DNNs, estimating the signal and ASE noise powers across an entire spectrum, no matter the spectral load configuration. We verify this approach through an experimental campaign, comparing the estimated end-of-line GSNR degradations to real QoT measurements. Our approach takes into account all nonlinear effects, stimulated Raman scattering (SRS), along with amplifier fluctuations induced by variations in the spectral load. We demonstrate the enhancements that result when combining an analytical QoT-E approach, in this case the GNPy engine, with a ML algorithm that provides an accurate GSNR prediction. Additionally, the approach taken within this work can be applied to next-generation SDN network management scenarios, pursuing an ultimate goal of a fully automated network without human input. As examples, we highlight an experimental implementation of an observe-decide-act (ODA) loop utilizing a ML algorithm performed in [46], [47], a tutorial showing how similar ML implementations may contribute to an automated network architecture in [48], along with a demo for a ML-based monitoring system for a fully disaggregated ROADM implementation in [49].

III. OPTICAL NETWORK ARCHITECTURE

In this work we consider a partially disaggregated optical network that operates within a SDN framework, where the amplified lines connecting ROADMs may be independent WDM OLSs [16], [17], [20], as pictorially described in Fig. 1. These ROADMs are operated in a disaggregated manner [4], [18], where each degree unit, including the wavelength selective switches (WSS)s are disaggregated, implying that different directions may be managed by independent OLSs. These ROADMs are assumed to be equipped with ASE noise generators that can be shaped by these WSSs for spectral noise loading, if required. Within the SDN architecture, each OLS is managed by an independent optical line controller (OLC) that sets the working points of the booster and preamp amplifiers included in the degree unit of the source and destination ROADMs, along with the in-line

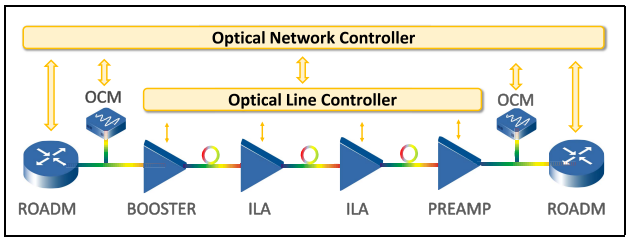

FIGURE 2. Conceptual schema of a ROADM-to-ROADM WDM optical line system. We suppose that the ROADM only includes the optical switching component and the booster and preamp amplifiers considered as part of the optical line.

amplifiers (ILAs). This OLC defines the amplifier working points and consequently the propagation impairments (as GSNR degradations) on each LP deployed on the line. All OLSs are assumed to be bidirectional and symmetric: for simplicity we refer to a single direction in figures and descriptions – these concepts are presented schematically in Fig. 2.

We suppose that the OLC operates in a way which is agnostic with respect to the traffic in the OLS, meaning that potentially unknown and proprietary algorithms may be in use. Additionally, we assume that a line model is supplied to the SDN optical network controller (ONC) by the OLC, for the purpose of network management [17], [18]. The ONC has overarching control over the entire network; in particular it controls the path of the optical tributary signals [19] through the WDM optical line systems on every ROADM-to-ROADM optical line, sets the switching matrices in ROADMs, and manages all control and safety operations [16], [18], [20]. Furthermore, the ONC has access to telemetry data that is retrieved from all monitors within the line. The ONC may read the outputs of the optical channel monitors (OCM)s at the ROADM I/Os [4] to get a per-channel power measurement, along with amplifier gain values from the amplifier I/Os.

When an optical tributary signal is requested, the ONC first defines the available routes and wavelengths in order to establish a transparent LP by running the routing and wavelength assignment (RWA) algorithm. Subsequently, the ONC runs the L-PCE that tests the actual QoT (the GSNR) on the defined LP. The RWA algorithm may work in conjunction with the L-PCE to enable a QoT-aware RWA. In general, the L-PCE pictorially described in Fig. 3 can be a closed module with standardized interfaces, and the proposed ML agent can be implemented as an add-on.

In this work, the L-PCE is implemented by relying on GNPy as a QoT-E. After defining the route from the source, s, to the destination, d, in the considered transparent infrastructure, the L-PCE requires the QoT-E to navigate the topological graph that abstracts the network WDM layer [50] and computes the overall GSNR_{sd}, which is given by:

$$\mathrm{GSNR}_{sd} = \frac{1}{\sum\limits_{i,j \in \mathrm{LP}_{sd}} \frac{1}{\mathrm{GSNR}_{ij}}}, \tag{1}$$

where i and j label, in turn, the OLS ROADM source and destination nodes crossed by the LP, and GSNR_{ij} are the respective GSNRs for the specified wavelength of the channel under test (CUT), λ_{CUT}. The ONC provides the line model and the OLS spectral load to the QoT-E, providing the GSNR_{ij}, expressed as follows:

$$\mathrm{GSNR}_{ij} = \frac{1}{\frac{1}{\mathrm{OSNR}_{ij}} + \frac{1}{\mathrm{SNR}_{\mathrm{NL},ij}}}, \tag{2}$$

where $\mathrm{OSNR}_{ij} = P_{\mathrm{CUT},ij}/P_{\mathrm{ASE},ij}$ and $\mathrm{SNR}_{\mathrm{NL},ij} = P_{\mathrm{CUT},ij}/P_{\mathrm{NLI},ij}$ are the optical SNR degradations from ROADM i to ROADM j due to the accumulated ASE noise, $P_{\mathrm{ASE},ij}$, and the NLI interference, $P_{\mathrm{NLI},ij}$, respectively. $P_{\mathrm{CUT},j}$ is the power of the channel under test at the input of the destination ROADM of OLS_{ij}. It has been proven that, if a precise line description is available, GNPy provides an extremely accurate GSNR computation, even for brownfield scenarios [12], [13] Nevertheless, amplifier characterizations are commonly given for a full spectral load scenario, for a given line description. Considering a progressive and varying spectral load scenario, for each OLS_{ij}, a non-trivial separation between the actual amplifier gain profile and noise figure and their nominal values are induced. Consequently, unpredictable and non-negligible fluctuations arise on both the OSNR_{ij} and the $\mathrm{SNR}_{\mathrm{NL},ij}$. A full characterization on the behaviour of these fluctuations would require, for each OLS, an enormous number of measurements of amplifier responses to different spectral load configurations, which scale linearly with the number of amplifiers and exponentially with the number of available channels on the specific OLS. Instead, we propose a ML approach that can be trained using a dataset that is obtained from each OLS_{ij}; for a given ASE noise generator within a given ROADM, it is possible to probe each OLS_{ij} of the network with different ASE-shaped spectral loads, collecting OCM measurements in the i and j ROADMs. These measurements are supplied to a DNN model that is used to evaluate the OSNR_{ij} in the L-PCE for specific spectral loads. This prediction can be combined with the $\mathrm{SNR}_{\mathrm{NL},ij}$ computation provided by the GNPy engine in order to obtain an overall QoT-E, as described in Fig. 3 option (b).

IV. EXPERIMENTAL SETUP

An experimental setup was created containing 9 commercial EDFAs and 8 fibers that are characterized by distinct physical parameters; a schematic block diagram is depicted in Fig. 4. Starting from the transmitter, the OLS begins with a booster amplifier that is set to produce a flat, constant power value of -1 dBm for each channel (regardless of the spectral load configuration), followed by 8 fiber spans, each approximately 80 km long, with a mixture of single mode fiber (SMF) types, each followed by a commercial EDFA [51] operating with distinct and constant gain and tilt values. To generate the input spectral loads, an ASE noise source has been manipulated using a commercial programmable WaveShaper© (1000S from Finisar) obtaining

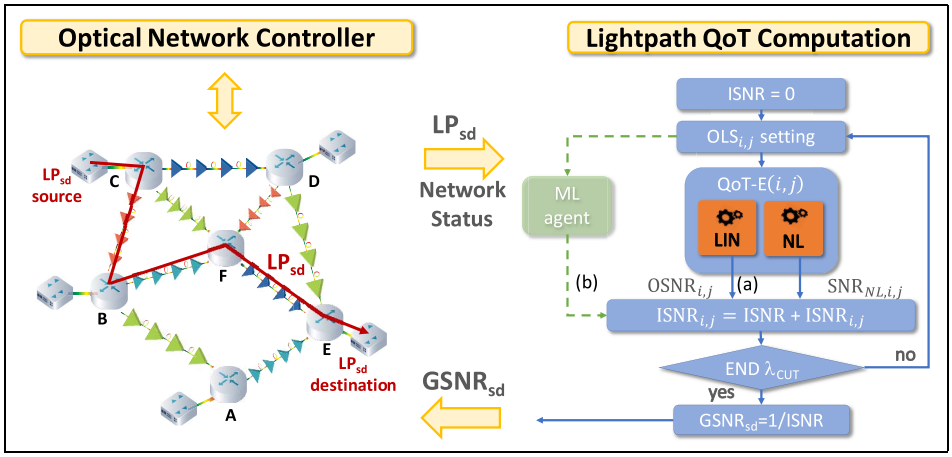

FIGURE 3. Schematic description of the L-PCE that enables QoT computation of a LP under test in a partially disaggregated optical network. In option (a) the GSNR is computed solely from the QoT-E, whereas in (b) the QoT-E computes the SNR_{NL} and the OSNR component is estimated using a ML algorithm. In this representation we abbreviate 1/GSNR as ISNR and separate the QoT-E outputs in linear, LIN, and nonlinear, NL, components.

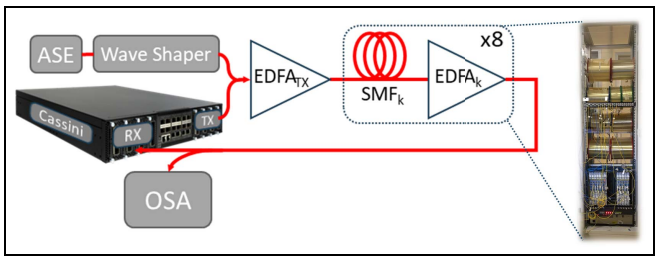

FIGURE 4. A schematic representation of the experimental setup described within this work.

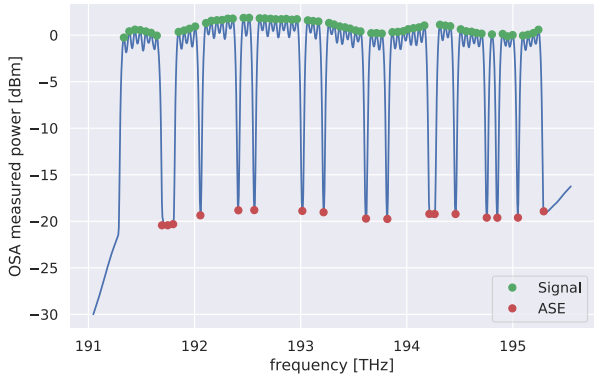

FIGURE 5. The power measured using the end-of-line OSA for one of the 2520 spectral load configurations. Channels which are turned on provide signal power measurements, whereas channels which are turned off provide ASE noise power measurements.

a 80 channel WDM comb, centered at 193.3 THz with a WDM grid spacing of 50 GHz within the C-band, according to ITU-T specifications [52]. We consider two CUTs, centered at 191.65 and 194.95 THz, that we refer to as CUT 7 and CUT 73, respectively, given their cardinal position in the WDM comb. For these CUTs, the signal transmission is managed by a commercial AS7716-24SC Cassini device [53], along with a CFP2-DCO coherent module from Lumentum, that is able to generate and detect either a 32 GBaud, quadrature phase shift keying (QPSK) modulated signal or a 43 GBaud, 8-quadrature amplitude modulated (8-QAM) modulated signal.

In order to control the settings of each EDFA, i.e., the gain and tilt values, software has been developed in the MATLAB environment. An optical spectrum analyzer (OSA) has been placed at the end of the OLS to emulate the OCM at the ROADM I/Os. Within this experimental framework, we generate 2520 different spectral loads, iterating through various scenarios where a different number of channels are turned on. In each scenario, permutations that represent unique spectral load configurations are generated, between a minimum of 2 channels turned on up to the maximum spectral load case of 80 channels. For each of these configurations, the power levels of all 80 channels are measured, obtaining the signal power if the channel is turned on and the ASE power if the channel is turned off; an example spectrum power measurement performed using the OSA is shown in Fig. 5. We assume that the four-wave mixing component of the NLI impairment is negligible for all OLS parameter configurations under investigation, as verified in [44], [54]. Furthermore, for all spectral load configurations we measure the BER in transmission associated with the specific CUT investigated. From these quantities we obtain a quantitative estimation of the GSNR by inverting the BER vs the OSNR curve, obtained through a progressive back-to-back noise loading characterization [13].

V. OPTICAL LINE SYSTEM CHARACTERIZATION

As mentioned in the previous sections, the GNPy engine requires a comprehensive description of the line model under test for QoT-E purposes. In particular, the physical parameters of the fiber spans were unknown before initiating the experimental campaign. As a preliminary analysis, we performed an optical time domain reflectometer (OTDR) analysis to probe the lengths and loss coefficients α of the

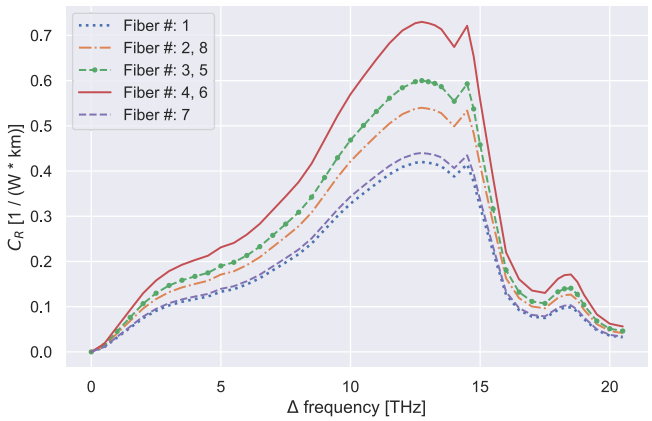

FIGURE 6. Final SRS efficiency curves deduced and used for each fiber span.

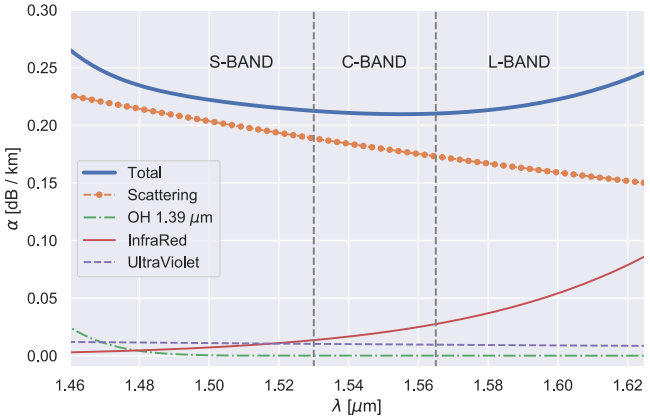

FIGURE 7. A generic loss coefficient profile and the related four model contributions.

TABLE 1. Fiber configurations tested within this experimental campaign.

#	$\bar{\alpha}$ [dB/km]	D [ps/(nm·km)]	C_R [(W·km)$^{-1}$]	L [km]
1	0.191	16.7	0.42	80.4
2	0.194	3.8	0.54	80.4
3	0.188	8.0	0.6	80.6
4	0.196	4.4	0.73	79.9
5	0.199	4.4	0.6	79.8
6	0.210	4.4	0.73	75.8
7	0.189	3.8	0.44	66.8
8	0.187	3.8	0.54	78.6

TABLE 2. EDFA configurations tested within this experimental campaign.

#	Gain [dB]	Tilt [dB]
0	19.8	0.2
1	16.9	1.4
2	16.5	1.4
3	17.9	1.4
4	19.1	1.4
5	18.7	1.4
6	17.3	1.6
7	18.7	1.4
8	20.6	1.4

fiber spans within the link at the OTDR pulse frequency (193.414 THz). After investigating the full dataset of these measurements, this characterization was found to not be sufficiently accurate, as the signal experienced a more severe frequency dependent tilt than expected. These discrepancies arise due to characterization inaccuracies of both the spectral fiber loss coefficient profile, initially considered flat in frequency, and the efficiency curve of the stimulated Raman scattering (SRS). To overcome this, we implemented an optimization algorithm that, given a model for both the fiber loss coefficient and the SRS efficiency, provides the joint characterization that best matches the experimental signal profile of the full spectrum scenario.

Regarding the SRS contribution, we consider a fixed, normalized efficiency curve [55] multiplied by a fiber span-dependent Raman coefficient, C_R, with the resulting SRS efficiency curves shown in Fig. 6. Regarding the frequency-dependent fiber loss coefficient profile, $\alpha_{dB/km}$, we adopt a model that takes into account a full description of the physical phenomena over the frequency range of interest. Starting from [56] and considering only the four main contributions that occur in the C-band, we obtain the following simplified model:

$$\alpha_{dB/km} \simeq \alpha_{\mathrm{S}} + \alpha_{\mathrm{UV}} + \alpha_{\mathrm{IR}} + \alpha_{13}\,, \tag{3}$$

where:

$$\begin{aligned}
\alpha_{\mathrm{S}} &= A\lambda^{-4} + B\,,\\
\alpha_{\mathrm{UV}} &= K_{\mathrm{UV}} e^{C_{\mathrm{UV}}/\lambda}\,,\\
\alpha_{\mathrm{IR}} &= K_{\mathrm{IR}} e^{-C_{\mathrm{IR}}/\lambda}\,,\\
\alpha_{13} &= A_1 \left(\frac{A_a}{A_1} e^{\frac{-(\lambda-\lambda_a)^2}{2\sigma_a^2}} + \frac{1}{A_1} \sum_{i=1}^{3} A_i e^{\frac{-(\lambda-\lambda_i)^2}{2\sigma_i^2}} \right),
\end{aligned}$$

are the Rayleigh scattering, ultraviolet, infrared and OH^- peak contributions, respectively. Considering these expressions in logarithmic units (dB/km), the Rayleigh scattering loss has a linear trend, the ultraviolet and the infrared absorption contributions have exponential forms and the OH^- peak absorption term, centered at 1.39 μm, may be approximated as a quadruple-Gaussian equation. As the ultraviolet absorption provides a constant contribution to the overall attenuation profile, this term has not been optimized. Consequently, Eq. 3 depends only upon four parameters; A, B, K_{IR}, A_1, providing a highly functional solution that allows even broadband fiber loss coefficient profiles to be derived easily.

In Fig. 7, we plot an example of the total $\alpha_{dB/km}$ and its separate contributions against wavelength, λ.

This approach allowed the fiber loss coefficient and SRS fiber efficiency values to be estimated to a satisfactory level of accuracy. Furthermore, the resulting SRS coefficients allow the different fiber types to be classified and enable distinct dispersion coefficients to be set. As the last required fiber parameter, we assume a single nonlinear coefficient value, $\gamma = 1.27\ \mathrm{W}^{-1}\cdot\mathrm{km}^{-1}$. We report the characterization results for all fibers within the OLS in Tab. 1. Regarding EDFA gain and tilt, we list the values used in this experimental campaign in Tab. 2. In general, we anticipate that

these values are fixed and may be retrieved from the OLC. The OLS characterizations described in this section were supplied to the GNPy engine in order to acquire a reference QoT-E.

VI. MACHINE LEARNING AIDED QOT-E

In this work we follow-up the approach presented in [44], implementing a ML algorithm that is able to enhance QoT computation over the OLS under investigation, reducing OSNR estimation inaccuracies. Firstly, we underline that the application of ML must be restricted to the OSNR contribution of the total GSNR, as the $\mathrm{SNR_{NL}}$ can only be measured if the channel transports a modulated signal. Subsequently, creating a training dataset that fulfils this condition before traffic deployment is unfeasible within the considered network framework. Moreover, various mathematical models (considering specifically the GN model), have been shown to provide a precise estimation of nonlinear effects due to fiber propagation, dependent upon certain physical parameters being given with to a required level of accuracy. In this framework a ML approach provides the greatest benefit when used to reduce uncertainties that are often accounted for simply through use of a design margin.

Such uncertainties include the aging of optical components, a lack of device characterizations, inaccuracies due to estimations made by proprietary software and fluctuations in the amplification process which are unaccounted for by the current model in question. It is worth noting that the ASE noise measurement described in Section IV, which is carried out when the channel is turned off, is a biased estimator of the actual ASE noise that affects the channel when it is turned on. Nevertheless, the bias in this prediction decreases significantly as the number of channels contributing to the spectral load increases – this value is always an overestimation that results in a conservative QoT prediction. As the spacing of the channels prevents measurement of the ASE noise within the channel frequency neighborhood, we highlight that the ASE noise may only be measured for a given channel when the channel is turned off.

Considering the ML algorithm implemented within this work, we normalize and divide the dataset into training, validation and testing subsets, making up 60%, 10% and 30% of the total dataset size, respectively. Using the open source TensorFlow© library, we implement a DNN model that consists of 4 hidden layers, each including 512 nodes; these values have been found to be optimal from the validation process, providing a satisfactory trade-off between the accuracy of the ML predictions and the overall training time. The computer used to run this training procedure contained a quad-core Intel Core i7-8565U CPU running at 1.80GHz, along with 8 GB of RAM, giving a total training time for each DNN of approximately 6 hours.

In order to estimate the OSNR, we train two distinct ML models, predicting the signal and ASE noise power levels,

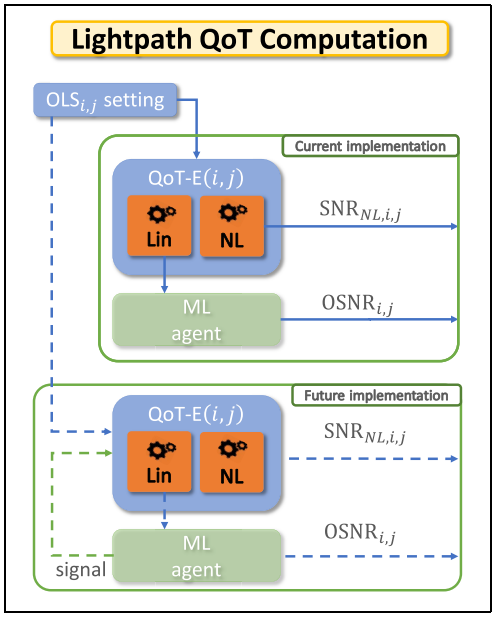

FIGURE 8. A description of the ML process used within this work; after the $\mathrm{OLS}_{i,j}$ settings are provided, the linear components (the signal and ASE noise powers) are supplied to the ML agent, whereas the NLI component is estimated using the GNPy engine. A future implementation scenario is also shown, described in Section VIII.

respectively. As the spectral load changes for every measurement within the dataset, it is important to choose a suitable set of features that serve as DNN inputs, as well as suitable outputs. Considering first the feature requirements, these must be fixed before the training process is started and cannot be changed once they have been chosen. These features used for the training stage must correspond to known system variables to obtain any individual prediction of the DNN outputs. Therefore, by exclusion, the entire set of power measurements can be used uniquely as DNN outputs, as they are not known for any individual spectral load. The only information that is known before a prediction is made are the channel statuses, which are either on or off. This information is relatively limited with respect to the entire realization space of both the signal and ASE power levels and leads to a low accuracy prediction.

In order to increase the DNN prediction performance we apply the following solution, presented diagrammatically in Fig. 8. Firstly, we supply the ML models with the array of channel statuses, along with the signal and the ASE noise predictions obtained using the GNPy engine – this enriches the input information, providing a partial insight of the OLS responses to specific spectral loads. Secondly, we perform the DNN training process over the entire spectral load, requesting information over all channels, not only the CUTs. As the number of channels varies between distinct spectral loads, we set the number of DNN outputs equal to the maximum number of available channels within the system under investigation. As the node weights are shared among the DNN outputs, specific channel predictions are tuned by considering the entire spectrum; consequently, precise

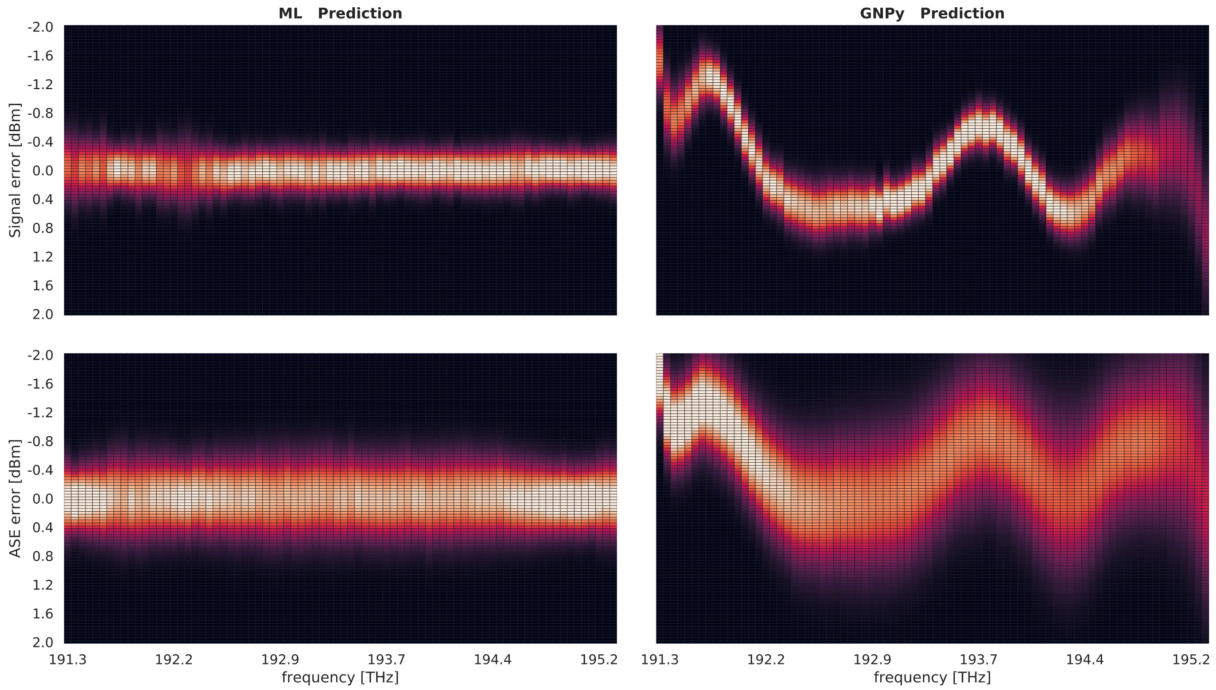

FIGURE 9. Error distribution of the signal and ASE noise prediction obtained with the the ML models and the GNPy engine, respectively.

information provided by the measurements is propagated through the entire DNN.

A straightforward issue is that when a channel is turned on, the signal power can be measured, however, the power of the ASE noise cannot. On the contrary, when a channel is turned off, by definition there is no signal power, but the ASE noise power can be measured. A naive solution is to set the unmeasured channel power quantities to zero during the training procedure. In our implementation we provide a better solution by taking advantage of the correlation between the spectral profiles of the signal and ASE noise power levels at the OLS output. In fact, both of these quantities are subject to the same gain and loss profiles during propagation and can be combined, constructing two unique, normalized and properly dimensioned power arrays that maximize the information supplied to the DNN. These two arrays of artificial quantities are used, respectively, for the prediction of the signal and ASE noise powers. Considering the signal power inputs and outputs, we take the array of signal powers and fill the missing elements with the rescaled ASE noise powers. For the ASE noise power inputs and outputs, we perform the opposite, replacing all missing elements with rescaled signal power values.

With this strategy, each DNN has a total of 160 inputs and 80 outputs; the inputs are composed of 80 channel statuses, combined with 80 power level estimates of ASE noise or signal power (depending upon the DNN model), whereas the outputs represent 80 power level values. Enhancing the ML implementation in this way enables accurate predictions of both the signal and ASE noise powers and hence a precise OSNR estimation to be obtained.

VII. RESULTS

In this section we present the ML prediction results that were obtained for a testing dataset containing 808 different spectral load configurations. As an accuracy metric, we evaluate the root-mean-square error (RMSE), which is defined with the following expression, for any pair of measured, X^m, and predicted, X^p, quantities:

$$\mathrm{RMSE}(X^m, X^p) = \sqrt{\frac{\sum_{i=0}^{N} \left(X_i^m - X_i^p\right)^2}{N}}, \tag{4}$$

where N is the total number of tested spectral load configurations. Alongside this metric, we define the error of a prediction as simply the difference between the measured and predicted quantities:

$$\Delta X = X^m - X^p . \tag{5}$$

As a first demonstration of the benefits in utilizing a ML approach, we investigate the DNN accuracy, estimating the signal and ASE noise power levels over the entire spectrum and compare them to the corresponding results obtained using the GNPy engine. Regarding the signal power predictions, RMSE values ranging between 0.2 and 1.5 dBm were found using the GNPy engine (depending upon the channel under investigation). Using instead a ML approach, the RMSE values ranged between 0.2 and 0.3 dBm, demonstrating an increase in prediction accuracy. Similarly, considering the ASE noise power predictions, the RMSE range prediction is reduced from 0.5 to 1.5 dBm to 0.3 to 0.4 dBm. A qualitative insight of this accuracy improvement is shown in Fig. 9, where the signal and ASE noise

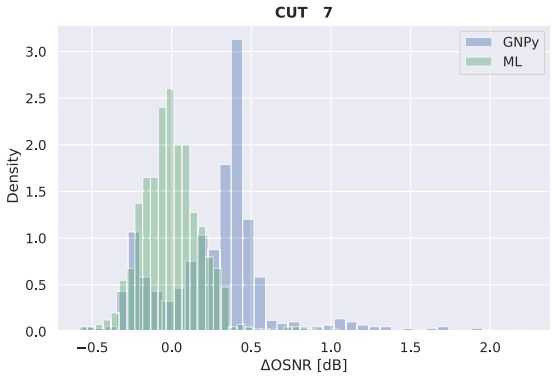

FIGURE 10. The error distribution for the OSNR predictions provided by the GNPy engine and the ML algorithm, for CUT 7.

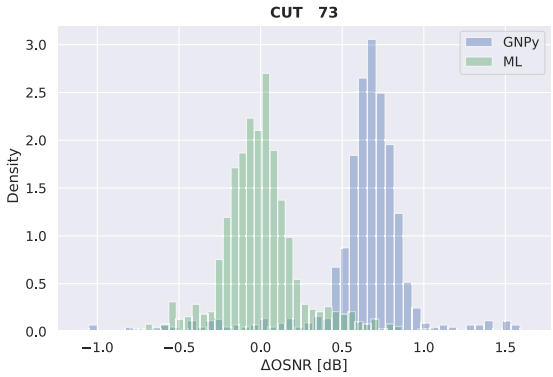

FIGURE 11. The error distribution for the OSNR predictions provided by the GNPy engine and the ML algorithm, for CUT 73.

results are reported for both prediction methods, illustrating the error distribution as a vertical colored strip for each channel, with brighter colors representing a higher distribution density, and vice versa. This figure serves as a qualitative visualization – the real error distributions have been replaced by equivalent Gaussian distributions with the same mean and standard deviation values. Nevertheless, Fig. 9 presents some interesting conclusions: firstly, applying ML moves the error distributions into a dense region of values concentrated around a zero mean, for both the signal and ASE noise power predictions, representing the best feature for a generic estimator. It is also visible that the higher RMSE values obtained using the GNPy engine are due to a biased estimation rather than incorrect modelling, as the error distributions maintain a limited standard deviation for every channel. This bias can be attributed to the fluctuations of the ILA responses to different spectral loads, which cannot be modelled in advance and consequently cannot be accounted for in the GNPy simulation. Moreover, the GNPy engine power predictions feature an increasing uncertainty as the characteristic spectral hole burning frequency (approximately 195 THz) is approached.

Beyond these observations, we next study how the aforementioned improvements affect the prediction of the signal-to-noise ratios. These quantities have been measured only for the CUTs, as they require a modulated signal, and in what follows we restrict our analysis to these two channels. As expected, through investigation of the dataset, we find that the covariance of the OSNR and $\mathrm{SNR_{NL}}$ is non-trivial. Therefore, in order to have a fair estimation of the enhancement provided by the ML approach, first we discuss the prediction accuracy of the OSNR. In Fig. 10 - 11 we report the error distributions of the OSNR predictions obtained with and without the ML models, for both CUTs. In this case, the ML methodology reduces the RMSE of the OSNR from 0.5 to 0.2 dB for CUT 7 and from 0.7 to 0.2 dB for CUT 73.

Finally, we investigate the final GSNR prediction obtained by applying the proposed methodology described in Fig. 8. In Fig. 12, we report the comparison between both the measured GSNR and fully predicted GSNR, and the ΔGSNR distributions for the two CUTs. Finally, the total RMSE value of the GSNR estimation is 0.3 dB for CUT 7 and 0.5 dB for CUT 73. Additionally, it can be observed in this case that the ML-aided prediction does not contain a bias for either of these CUTs. As the same behaviour is expected across the entire spectrum, it is possible to set a margin that yields conservative results in most cases. However, this feature is not guaranteed when using the GNPy engine due to the aforementioned estimation biases for the signal and ASE noise power predictions – this prevents a fixed margin, and hence a conservative result from always being reached. In this work, we applied a margin of 0.5 dB to the obtained predictions, shifting the error distributions as shown in Fig. 12; the error is calculated using Eq. (5), with positive values of this quantity representing conservative GSNR estimations. We remark that a margin of this size does not significantly affect the accuracy of the final predictions and is reduced with respect to most currently employed design margins [14]. This procedure provides a 90.5% and 94.6% conservative GSNR prediction for CUTs 7 and 73, respectively. Moreover, a margin such as this may also be defined to take into account additional SNR degradations, for example filtering penalties, which is a promising avenue for future investigations.

VIII. CONCLUSION

In this work, we consider a partially disaggregated optical network and aim to compute the QoT for LPs with dynamic traffic loading. We propose a methodology based around training a ML agent to assist QoT-E within the L-PCE to better model fluctuations in the ILA response behaviour under different spectral loads. To test the proposed solution, we carried out an experimental campaign that considers a non-transparent, point-to-point optical amplified line based on commercial amplifiers. Using this setup we measured the end-of-line GSNR over 2520 different spectral load configurations for two different CUTs. We show that, even if the full spectral load behavior can be accurately modelled, the GNPy engine is not able to predict the GSNR fluctuations that arise from unpredictable ILA responses. The result is an uncertainty in the GSNR prediction, which leads to deployment of significant margins. To reduce these uncertainties

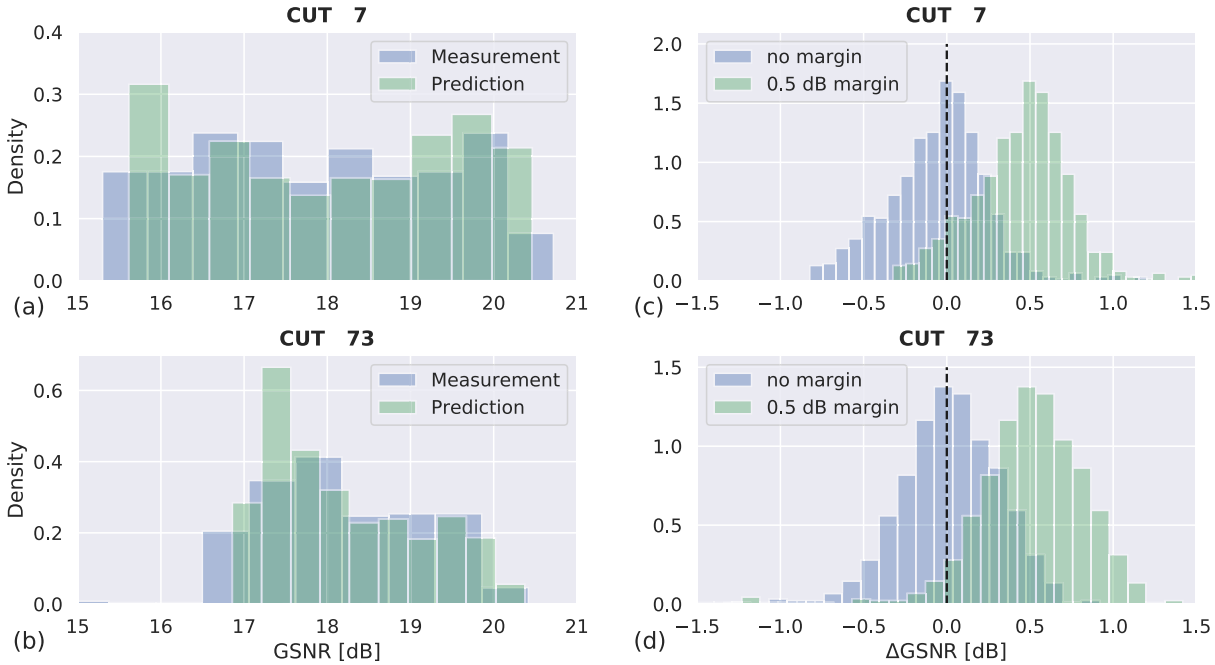

FIGURE 12. The measured and predicted GSNR power distributions for: (a) CUT 7 and (b) CUT 73, along with the corresponding ΔGSNR power distributions with and without a 0.5 dB margin for: (c) CUT 7 and (d) CUT 73.

and hence enable a reliable QoT estimation, we propose and verify the combined usage of a ML algorithm and the GNPy engine. The signal and ASE noise powers are estimated using the GNPy engine; these results are then supplied to the ML algorithm for the ML training procedure, as shown in Fig. 8, in order to obtain the most accurate OSNR predictions. After the ML models have been trained, we combine these OSNR predictions with SNR_{NL} estimations provided by the GNPy engine, obtaining accurate final GSNR evaluations, for the entire set of tested spectral load configurations. We show that, by including a system margin of 0.5 dB, more the 90% of the predictions are conservative, without significantly affecting the accuracy of our results. Moreover, we highlight that the ML models perform well when predicting both the signal and ASE noise power levels for all channels. The separate estimation of these two quantities can be used to optimize the OLS settings, further increasing the accuracy of the proposed QoT-E and improving the SNR_{NL} predictions, shown in Fig. 8 as a future implementation.

We remark that the proposed solution is completely agnostic with respect to both the hardware and the control strategy, as it only requires ASE-shaped generators and measurements from the OCMs, both commonly available in ROADM I/Os, in order to create a ML training dataset. Consequently, the solution which we propose is demonstrated to be a feasible and non-intrusive method for L-PCE accuracy improvement, allowing a seamless increase in network performance.

ACKNOWLEDGMENT

The authors wish to thank the Telecom Infra Project, EdgeCore, Lumentum, Cisco and IP Infusion for providing hardware and software used for the experiments detailed within this work.

REFERENCES

[1] Cisco. (2018). *Cisco Visual Networking Index: Forecast and Methodology*. Accessed: Jan. 14, 2021. [Online]. Available: https://www.cisco.com/c/en/us/solutions/service-provider/visual-networking-index-vni/index.html

[2] D. J. Ives, P. Bayvel, and S. J. Savory, "Routing, modulation, spectrum and launch power assignment to maximize the traffic throughput of a nonlinear optical mesh network," *Photon. Netw. Commun.*, vol. 29, no. 3, pp. 244–256, 2015.

[3] V. Curri, M. Cantono, and R. Gaudino, "Elastic all-optical networks: A new paradigm enabled by the physical layer. How to optimize network performances?" *J. Lightw. Technol.*, vol. 35, no. 6, pp. 1211–1221, Mar. 15, 2017.

[4] J. Kundrát, O. Havliš, J. Jedlinskỳ, and J. Vojtěch, "Opening up roadms: Let us build a disaggregated open optical line system," *J. Lightw. Technol.*, vol. 37, no. 16, pp. 4041–4051, Aug. 15, 2019.

[5] M. Gunkel *et al.*, "Vendor-interoperable elastic optical interfaces: Standards, experiments, and challenges," *J. Opt. Commun. Netw.*, vol. 7, no. 12, pp. B184–B193, 2015.

[6] M. Filer, H. Chaouch, and X. Wu, "Toward transport ecosystem interoperability enabled by vendor-diverse coherent optical sources over an open line system," *IEEE/OSA J. Opt. Commun. Netw.*, vol. 10, no. 2, pp. A216–A224, Feb. 2018.

[7] J.-L. Auge, G. Grammel, E. Le Rouzic, V. Curri, G. Galimberti, and J. Powell, "Open optical network planning demonstration," in *Proc. Opt. Fiber Commun. Conf.*, 2019, pp. 3–9.

[8] M. Filer, M. Cantono, A. Ferrari, G. Grammel, G. Galimberti, and V. Curri, "Multi-vendor experimental validation of an open source QoT estimator for optical networks," *J. Lightw. Technol.*, vol. 36, no. 15, pp. 3073–3082, Aug. 1, 2018.

[9] A. Bononi, P. Serena, and N. Rossi, "Nonlinear signal–noise interactions in dispersion-managed links with various modulation formats," *Opt. Fiber Technol.*, vol. 16, no. 2, pp. 73–85, 2010.

[10] P. Poggiolini, A. Carena, Y. Jiang, G. Bosco, V. Curri, and F. Forghieri, "Impact of low-OSNR operation on the performance of advanced coherent optical transmission systems," in *Proc. IEEE Eur. Conf. Opt. Commun. (ECOC)*, 2014, pp. 1–3.

[11] *GitHub Repository of GNPy*. Accessed: Feb. 18, 2021. [Online]. Available: https://doi.org/10.5281/zenodo.3458319

[12] A. Ferrari *et al.*, "Experimental validation of an open source quality of transmission estimator for open optical networks," in *Proc. IEEE Opt. Fiber Commun. Conf. Exhibit. (OFC)*, 2020, pp. 1–3.

[13] A. Ferrari *et al.*, "GNPY: An open source application for physical layer aware open optical networks," *J. Opt. Commun. Netw.*, vol. 12, no. 6, pp. C31–C40, 2020.

[14] P. Soumplis, K. Christodoulopoulos, M. Quagliotti, A. Pagano, and E. Varvarigos, "Network planning with actual margins," *J. Lightw. Technol.*, vol. 35, no. 23, pp. 5105–5120, Dec. 1, 2017.

[15] Y. Pointurier, "Design of low-margin optical networks," *IEEE/OSA J. Opt. Commun. Netw.*, vol. 9, no. 1, pp. A9–A17, Jan. 2017.

[16] S. Gringeri, B. Basch, V. Shukla, R. Egorov, and T. J. Xia, "Flexible architectures for optical transport nodes and networks," *IEEE Commun. Mag.*, vol. 48, no. 7, pp. 40–50, Jul. 2010.

[17] C. Manso *et al.*, "Tapi-enabled SDN control for partially disaggregated multi-domain (OLS) and multi-layer (WDM over SDM) optical networks," *J. Opt. Commun. Netw.*, vol. 13, no. 1, pp. A21–A33, 2021.

[18] M. Birk *et al.*, "The openroadm initiative," *IEEE/OSA J. Opt. Commun. Netw.*, vol. 12, no. 6, pp. C58–C67, Jun. 2020.

[19] *G.807: Generic Functional Architecture of the Optical Media Network*. Accessed: Feb. 18, 2021. [Online]. Available: https://www.itu.int/rec/T-REC-G.807-202002-I/en

[20] E. Riccardi, P. Gunning, Ó. G. de Dios, M. Quagliotti, V. López, and A. Lord, "An operator view on the introduction of white boxes into optical networks," *J. Lightw. Technol.*, vol. 36, no. 15, pp. 3062–3072, Aug. 2018.

[21] V. Curri *et al.*, "Design strategies and merit of system parameters for uniform uncompensated links supporting nyquist-WDM transmission," *J. Lightw. Technol.*, vol. 33, no. 18, pp. 3921–3932, Sep. 15, 2015.

[22] A. Ferrari, G. Borraccini, and V. Curri, "Observing the generalized SNR statistics induced by gain/loss uncertainties," in *Proc. IEEE Eur. Conf. Opt. Commun. (ECOC)*, 2019, pp. 1–9.

[23] B. Taylor, G. Goldfarb, S. Bandyopadhyay, V. Curri, and H.-J. Schmidtke, "Towards a route planning tool for open optical networks in the telecom infrastructure project," in *Proc. Opt. Fiber Commun. Conf. Nat. Fiber Opt. Eng. Conf.*, 2018, pp. 1–3.

[24] M. Bolshtyansky, "Spectral hole burning in erbium-doped fiber amplifiers," *J. Lightw. Technol.*, vol. 21, no. 4, pp. 1032–1038, Apr. 2003.

[25] T. Jiménez *et al.*, "A cognitive quality of transmission estimator for core optical networks," *J. Lightw. Technol.*, vol. 31, no. 6, pp. 942–951, Mar. 15, 2013.

[26] L. Barletta, A. Giusti, C. Rottondi, and M. Tornatore, "Qot estimation for unestablished lighpaths using machine learning," in *Proc. Opt. Fiber Commun. Conf.*, 2017, pp. 1–2.

[27] C. Rottondi, L. Barletta, A. Giusti, and M. Tornatore, "Machine-learning method for quality of transmission prediction of unestablished lightpaths," *J. Opt. Commun. Netw.*, vol. 10, no. 2, pp. A286–A297, 2018.

[28] I. Sartzetakis, K. K. Christodoulopoulos, and E. M. Varvarigos, "Accurate quality of transmission estimation with machine learning," *J. Opt. Commun. Netw.*, vol. 11, no. 3, pp. 140–150, 2019.

[29] P. Samadi, D. Amar, C. Lepers, M. Lourdiane, and K. Bergman, "Quality of transmission prediction with machine learning for dynamic operation of optical WDM networks," in *Proc. IEEE Eur. Conf. Opt. Commun. (ECOC)*, 2017, pp. 1–3.

[30] R. M. Morais and J. Pedro, "Machine learning models for estimating quality of transmission in DWDM networks," *J. Opt. Commun. Netw.*, vol. 10, no. 10, pp. D84–D99, 2018.

[31] F. Musumeci *et l.*, "An overview on application of machine learning techniques in optical networks," *IEEE Commun. Surveys Tuts.*, vol. 21, no. 2, pp. 1383–1408, 2nd Quart., 2018.

[32] J. Mata *et al.*, "Artificial intelligence (AI) methods in optical networks: A comprehensive survey," *Opt. Switch. Netw.*, vol. 28, pp. 43–57, Apr. 2018.

[33] F. N. Khan, Q. Fan, C. Lu, and A. P. T. Lau, "An optical communication's perspective on machine learning and its applications," *J. Lightw. Technol.*, vol. 37, no. 2, pp. 493–516, Jan. 15, 2019.

[34] S. Zhu, C. L. Gutterman, W. Mo, Y. Li, G. Zussman, and D. C. Kilper, "Machine learning based prediction of erbium-doped fiber WDM line amplifier gain spectra," in *Proc. Eur. Conf. Opt. Commun. (ECOC)*, 2018, pp. 1–3.

[35] M. Ionescu, "Machine learning for ultrawide bandwidth amplifier configuration," in *Proc. IEEE 21st Int. Conf. Transp. Opt. Netw. (ICTON)*, 2019, pp. 1–4.

[36] E. D. A. Barboza, C. J. Bastos-Filho, J. F. Martins-Filho, U. C. de Moura, and J. R. de Oliveira, "Self-adaptive erbium-doped fiber amplifiers using machine learning," in *Proc. SBMO/IEEE MTT-S Int. Microwave Optoelectron. Conf. (IMOC)*, 2013, pp. 1–5.

[37] E. Seve, J. Pesic, and Y. Pointurier, "Accurate QoT estimation by means of a reduction of EDFA characteristics uncertainties with machine learning," in *Proc. Int. Conf. Opt. Netw. Design Model. (ONDM)*, 2020, pp. 1–3.

[38] M. Freire, S. Mansfeld, D. Amar, F. Gillet, A. Lavignotte, and C. Lepers, "Predicting optical power excursions in erbium doped fiber amplifiers using neural networks," in *Proc. IEEE Asia Commun. Photon. Conf. (ACP)*, 2018, pp. 1–3.

[39] Y. Huang *et al.*, "Dynamic mitigation of edfa power excursions with machine learning," *Opt. Exp.*, vol. 25, no. 3, pp. 2245–2258, 2017.

[40] A. Mahajan, K. Christodoulopoulos, R. Martinez, S. Spadaro, and R. Munoz, "Machine learning assisted EDFA gain ripple modelling for accurate QoT estimation," in *Proc. Eur. Conf. Opt. Commun. (ECOC)*, 2019, pp. 1–8.

[41] A. Mahajan, K. Christodoulopoulos, R. Martínez, S. Spadaro, and R. Muñoz, "Modeling EDFA gain ripple and filter penalties with machine learning for accurate QoT estimation," *J. Lightw. Technol.*, vol. 38, no. 9, pp. 2616–2629, May 2020.

[42] S. Zhu *et al.*, "Hybrid machine learning EDFA model," in *Proc. Opt. Fiber Commun. Conf.*, 2020, pp. 1–4.

[43] S. Aladin and C. Tremblay, "Cognitive tool for estimating the qot of new lightpaths," in *Proc. Opt. Fiber Commun. Conf.*, 2018, pp. 1–3.

[44] A. D'Amico *et al.*, "Using machine learning in an open optical line system controller," *J. Opt. Commun. Netw.*, vol. 12, no. 6, pp. C1–C11, 2020.

[45] *Tensorflow*. Accessed: Feb. 18, 2021. [Online]. Available: https://www.tensorflow.org/

[46] K. Christodoulopoulos *et al.*, "Toward efficient, reliable, and autonomous optical networks: The orchestra solution," *IEEE/OSA J. Opt. Commun. Netw.*, vol. 11, no. 9, pp. C10–C24, Sep. 2019.

[47] R. M. Morais, "Machine learning in multi-layer optical networks," in *Proc. Opt. Fiber Commun. Conf.*, 2020, p. 1.

[48] D. Rafique and L. Velasco, "Machine learning for network automation: Overview, architecture, and applications [invited tutorial]," *J. Opt. Commun. Netw.*, vol. 10, no. 10, pp. D126–D143, Oct. 2018. [Online]. Available: http://jocn.osa.org/abstract.cfm?URI=jocn-10-10-D126

[49] A. Sgambelluri *et al.*, "Fully disaggregated roadm white box with netconf/yang control, telemetry, and machine learning-based monitoring," in *Proc. Opt. Fiber Commun. Conf.*, 2018, pp. 1–12.

[50] V. Curri, "Software-defined wdm optical transport in disaggregated open optical networks," in *Proc. 22nd Int. Conf. Transp. Opt. Netw. (ICTON)*, 2020, pp. 1–4.

[51] *Cisco*. Accessed: Feb. 18, 2021. [Online]. Available: https://www.cisco.com/c/en/us/products/collateral/optical-networking/ons-15454-series-multiservice-transport-platforms/data_sheet_c78-658542.html

[52] "Series G: Transmission systems and media, digital systems and neTWORKS—Transmission media characteristics—Characteristics of optical components and subsystems—Spectral grids for WDM applications: DWDM frequency grid," ITU, Geneva, Switzerland, ITU-T Recommendation G.694.1, 2002, Accessed: Jan. 14, 2021. [Online]. Available: https://www.itu.int/rec/T-REC-G.694.1/en

[53] *Edge-Core*. Accessed: Feb. 18, 2021. [Online]. Available: https://www.edge-core.com/productsList.php?cls=291&cls2=347

[54] E. Virgillito, A. D'Amico, A. Ferrari, and V. Curri, "Observing and modeling wideband generation of non-linear interference," in *Proc. 21st Int. Conf. Transp. Opt. Netw. (ICTON)*, 2019, pp. 1–4.

[55] J. Bromage, "Raman amplification for fiber communications systems," *J. Lightw. Technol.*, vol. 22, no. 1, pp. 79–93, Jan. 2004.

[56] S. Walker, "Rapid modeling and estimation of total spectral loss in optical fibers," *J. Lightw. Technol.*, vol. 4, no. 8, pp. 1125–1131, Aug. 1986.